

## Supplementary Information

for

### Characteristics and Mechanisms of Dissolved Organic Matter Leached by Photodegradation of Polyethylene Microplastics: Role of adsorbed antibiotics

Yanan Chen<sup>b</sup>, Yunkun Qian<sup>\*ad</sup>, and Fan Liu<sup>c</sup>

a College of Environmental Science & Engineering, DongHua University, Shanghai 200051, P.R. China

b Department of Chemistry, Carnegie Mellon University, Pittsburgh, Pennsylvania 15213, United States

c Department of the Built Environment, Aalborg University, Thomas Manns Vej 23, Aalborg, Denmark

d Key Laboratory of Yangtze River Water Environment, Ministry of Education , China

Corresponding author: [qianyunkun@dhu.edu.cn](mailto:qianyunkun@dhu.edu.cn)

**Text 1 Average pore width and average specific surface area of PE-75  $\mu\text{m}$**

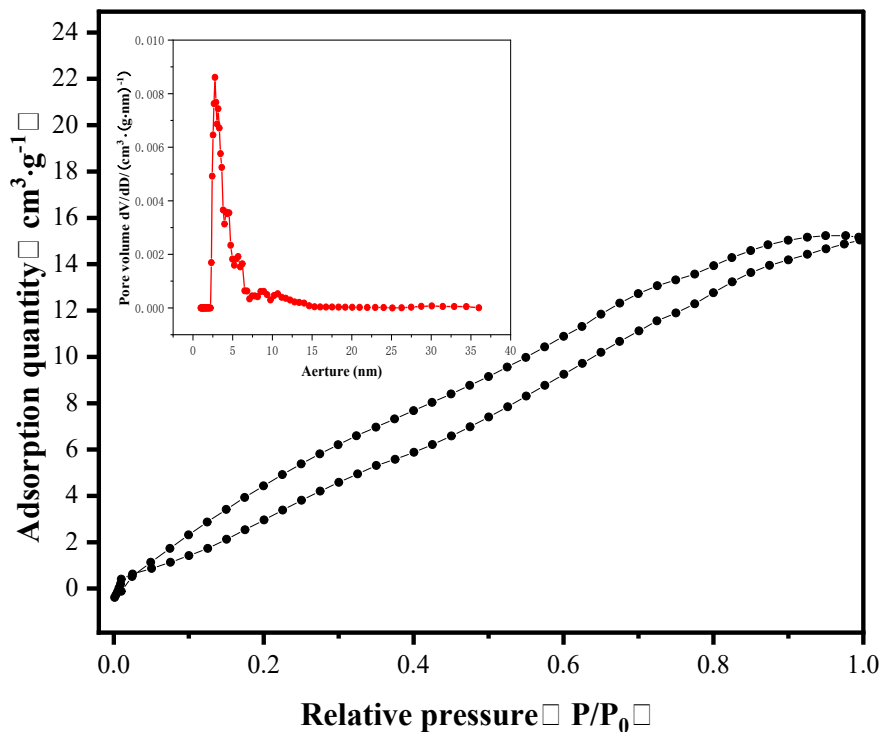


**Fig. S1.**  $\text{N}_2$  adsorption isotherm of PE-75  $\mu\text{m}$  particles (inset shown the pore size distribution).

**Text 2 Adsorption experiment**

Ofloxacin (OFL) were dissolved in deionized water for the preparation of 100 mg/L stock solution and kept in the dark at 4 °C. Batch adsorption experiments were designed as follows: 20 mg of PE particles (75  $\mu\text{m}$ ) and 20 mL of 500  $\mu\text{g}/\text{L}$  OFL solutions were added into 50 mL Erlenmeyer flasks. Then all samples were placed in a thermostatic shaker (Shanghai Tianhe Automation Instrumentation, Shanghai, China) and shaken at 160 rpm in the dark at 25 °C for 48 h to reach adsorption equilibrium. The use of 500  $\mu\text{g}/\text{L}$  OFL was intended to rapidly achieve adsorption saturation on the MPs, ensuring that the subsequent leaching experiments proceeded under saturated and controlled conditions. The adsorption process of OFL on PE-75  $\mu\text{m}$  are shown in Fig.S1. After the reaction, the mixed solution was filtered through 0.45  $\mu\text{m}$  filters for the analysis of residual OFL concentrations. The adsorption

saturated PE-75  $\mu\text{m}$  were collected for leaching experiments.

As shown in Fig. S5 and Fig. 1, only 56  $\mu\text{g/L}$  of DOM was released in the dark, whereas pristine PE generated more than 900  $\mu\text{g/L}$  after 2 days of UV exposure. This means that pre-leached DOM accounts for only 6% of the DOM produced at the onset of photodegradation. Therefore, the influence of DOM released during the adsorption step on the subsequent DOM leaching can be considered negligible.

The potential contribution of OFL-derived products to the total DOM pool in PE-OFL leaching experiments was evaluated as follows:

The initial OFL concentration in the PE-OFL system was 500  $\mu\text{g/L}$ . The adsorption capacity of PE for OFL is low, at 0.41  $\mu\text{g}$  OFL per mg PE (Fig. S2). For a typical experiment with 500 mg PE/L, this corresponds to a total of 205  $\mu\text{g}$  OFL adsorbed onto the particles. Even assuming conservatively that all 5% of degraded OFL (i.e., 5% of 200  $\mu\text{g}$  = 10.25  $\mu\text{g}$ ) were converted into “DOM-like substances” and released into the 1 L solution, the maximum possible contribution from OFL degradation would be 10.25  $\mu\text{g/L}$ .

This calculated maximum of 10.25  $\mu\text{g/L}$  is negligible compared to the thousands of  $\mu\text{g/L}$  of DOM leached from the PE matrix under UV irradiation (1889  $\mu\text{g/L}$  from PE-OFL at 14 d, Fig. 1). It represents less than 0.5% of the total DOM measured.

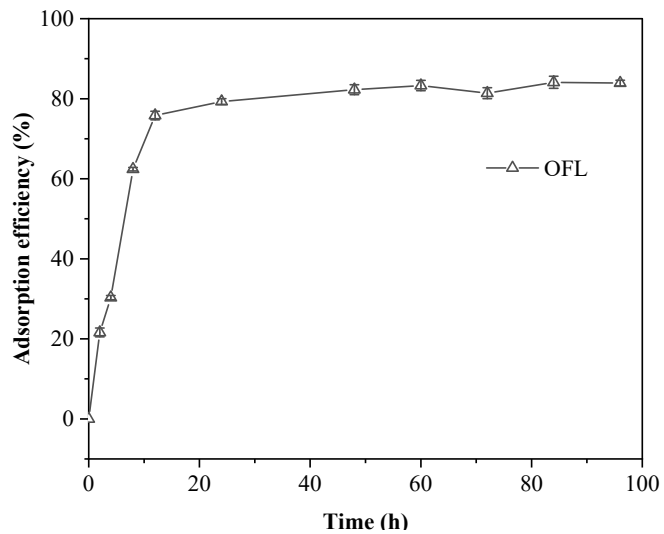


**Fig. S2.** Adsorption efficiency of OFL on PE with increasing reaction time.

**Text 3 Schematic diagram of UV reactor and Calculation of simulated sunlight exposure equivalent**

According to Gewert et al.,<sup>1</sup> the simulated sunlight exposure equivalent to European mean solar irradiance was calculated using the following formulas:

(1) European mean irradiance  $\approx 1200 \text{ kWh}/(\text{m}^2 \cdot \text{year})$

(2) 5 % of this is UV light: mean European UV irradiance =  $60 \text{ kWh}/(\text{m}^2 \cdot \text{year})$

(3) Total irradiance exposed [ $\text{Wh}/\text{m}^2$ ] = intensity (UV) [ $\text{W}/(\text{m}^2)$ ]  $\cdot$  hours of exposure [h]

(4) Simulated days = total irradiance exposed / mean European UV irradiance  $\cdot$  365

In our experiments, the distance between the light source and liquid level was 15 cm. The UV light intensity on the surface of the water samples was  $25 \text{ mW}/\text{cm}^2$  as measured by a radiometer (TES1333, TES Electrical Electronic Corporation, China). Thus, the calculation of simulated sunlight exposure equivalent as follows:

Total irradiance exposed:  $250 \text{ W}/\text{m}^2 \cdot 24\text{h} \cdot 14 = 84 \text{ kWh}/\text{m}^2$

Simulated days:  $84 \text{ kWh}/\text{m}^2 / 60 \text{ kWh}/\text{m}^2 \cdot \text{year}^{-1} \cdot 365 = 511 \text{ days}$

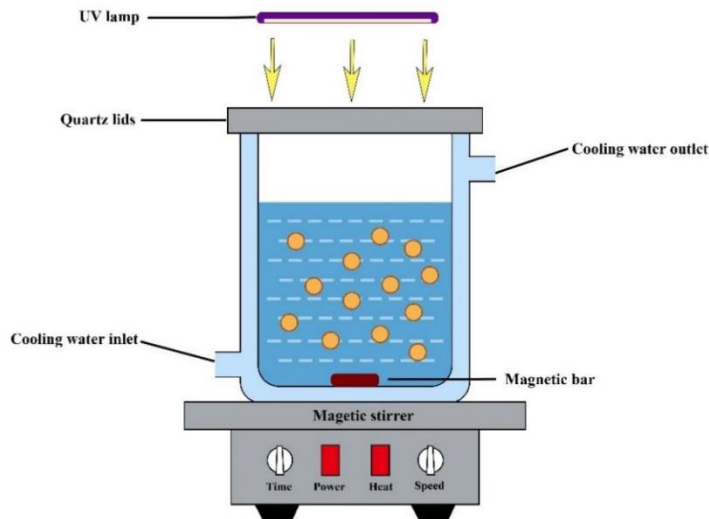


**Fig. S3.** Schematic diagram of UV reactor.

#### Text 4 MW fractionation

DOM samples were fractionated into MW < 1 kDa fractions by a Minimate™ II tangential flow filtration (TFF) system (Pall Corporation, USA) using Ultracel®-PL UF membranes (MilliporeSigma, USA) with nominal MW limits of 1 kDa, respectively. Before the fractionation, the UF membranes were rinsed and soaked for 30 min with deionized water. Then water samples were filtered successively by 1 kDa UF membranes. The serial processes in the Tangential Flow Filtration (TFF) system are shown in Fig. S4. DOC was measured for fractionated- and raw-water samples. The concentrations in different MW fractions were obtained by subtraction.

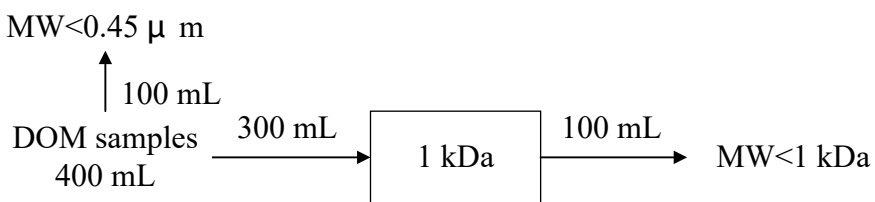


**Fig. S4.** Serial processes in the tangential flow filtration system.

#### Text 5 XPS analysis

X-ray photoelectron spectroscopy (XPS, K-Alpha, Thermo Scientific, USA) was used to acquire

wide-scan and high-resolution spectra of MPs, with a scanning range of 300–3000 eV and a step size of 0.1 eV. The C 1s peak at 284.6 eV was used as a reference for binding energy calibration. The full XPS spectrum was acquired using a pass energy of 100 eV, while narrow scans of target elements (C, O, N, F) were conducted with a pass energy of 100 eV with 5 acquisition cycles.

Data analysis and processing were performed using the XPSPeak 4.1 software with the Shirley-type background. All peaks were fitted using a mixed Gaussian-Lorentzian (GL(30)) line shape, and the O 1s XPS spectra were deconvoluted into three symmetric Lorentzian-Gaussian components: Peak I (531.6 eV) corresponds to C=O bonds in carboxyl, aldehyde, and ketone functionalities; Peak II (532.01 eV) to C-O bonds in hydroxyl and alcoholic; and Peak III (534.0 eV) to O-C-O linkages in alkyl peroxides and hydrogen peroxide derivatives. During fitting, FWHM was constrained to 1.5 eV, and peak position shifts were restricted to within  $\pm 0.3$  eV, while the relative peak areas were allowed to vary freely. Residuals from the fitted curves were examined to ensure the quality of deconvolution ( $\chi^2=8.3$ ), and no systematic deviations were observed.

**Text 6 Concentration of DOM leached from PE under dark and natural sunlight**

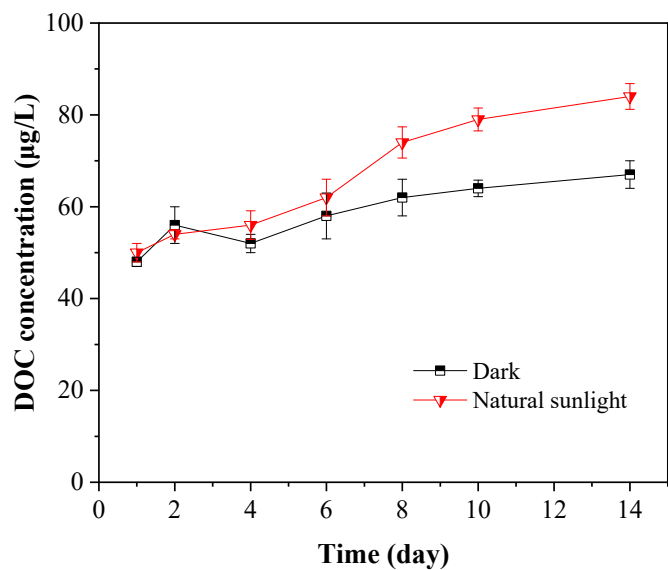


**Fig. S5.** DOC concentrations of DOM leached from (a) PE (0.5 g-PE/L) under dark and natural sunlight.

Text 7 Morphology of PE particles under original and UV exposure

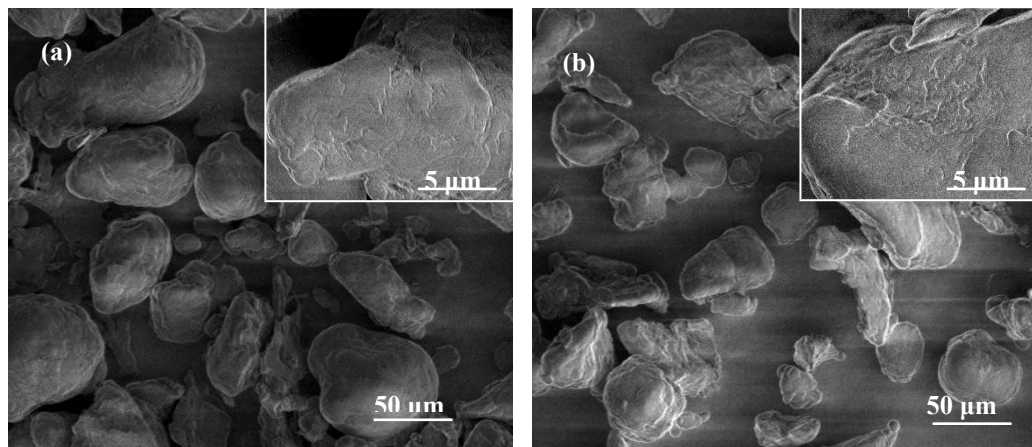


**Fig. S6.** Scanning electron microscopy of original (a) and 14 days of UV-exposure (b) PE microplastic particles.

**Text 8 Response sequence of functional groups in MPs-DOM**

**Table S4. 2DCOS of SF spectra results on the assignment and sign of each cross-peak in synchronous ( $\alpha$ ) and asynchronous ( $\beta$ , in parentheses) maps of IOM reaction with chlorine**

Location (nm)	Assignment	280	315–320	380	Sign <sup>a</sup>
280	tryptophan-like fluorescence fraction	+			
315–320	fulvic-like fluorescence fraction	+ (-)	+		
380	humic-like fluorescence fraction	+ (-)	+ (-)	+	

<sup>a</sup>Signs were obtained in the lower-right corner of the maps: +, positive; -, negative

## References

L. Bai, Z. Zhao, C. Wang, C. Wang, X. Liu, H. Jiang, Multi-spectroscopic investigation on the complexation of tetracycline with dissolved organic matter derived from algae and macrophyte. *Chemosphere*, 2017, **187**, 421–429.

W. Chen, N. Habibul, X. Liu, G. Sheng, H. Yu, FTIR and synchronous fluorescence heterospectral two dimensional correlation analyses on the binding characteristics of copper onto dissolved organic matter. *Environ. Sci. Technol.*, 2015, **49**, 2052–2058.

B. Hu, P. Wang, C. Wang, J. Qian, T. Bao, Y. Shi, Investigating spectroscopic and copper-binding characteristics of organic matter derived from sediments and suspended particles using EEM-PARAFAC combined with two-dimensional fluorescence/FTIR correlation analyses. *Chemosphere*, 2019, **219**, 45–53.

I. Noda, Y. Ozaki, Two-dimensional Correlation Spectroscopy: Applications in Vibrational and Optical Spectroscopy. *John Wiley & Sons, Ltd.*, 2005.

S. Xue, K. Wang, Q. Zhao, L. Wei, Chlorine reactivity and transformation of effluent dissolved organic fractions during chlorination. *Desalination*, 2009, **249**(1), 63–71.

G. Yu, M. Wu, G. Wei, Y. Luo, W. Ran, B. Wang, J. Zhang, Q. Shen, Binding of organic ligands with Al(III) in dissolved organic matter from soil: implications for soil organic carbon storage. *Environ. Sci. Technol.*, 2012, **46**(11), 6102–6109.

T. Zhou, A. Zhang, C. Zhao, H. Liang, Z. Wu, J. Xia, Molecular chain movements and transitions of SEBS above room temperature studied by moving window two-dimensional correlation infrared spectroscopy. *Macromolecules*, 2007, **40**, 9009–9017.